Wolf-Rayet Stars
W.-R. Hamann, A. Sander, H. Todt, eds.
Potsdam: Univ.-Verlag, 2015
URL: http://nbn-resolving.de/urn:nbn:de:kobv:517-opus4-84268

Properties of LEGUS Clusters Obtained with Different Massive-Star Evolutionary Tracks.

A. Wofford[1], S. Charlot[1] & J. J. Eldridge[2]
[1] *Institut d'Astrophysique de Paris, CNRS, UMR 7095, Sorbonne Universités, UPMC Univ Paris 6, France*
[2] *University of Auckland, New Zealand*

We compute spectral libraries for populations of coeval stars using state-of-the-art massive-star evolutionary tracks that account for different astrophysics including rotation and close-binarity. Our synthetic spectra account for stellar and nebular contributions. We use our models to obtain $E(B-V)$, age, and mass for six clusters in spiral galaxy NGC 1566, which have ages of < 50 Myr and masses of $> 5\times10^4\ M_\odot$ according to standard models. NGC 1566 was observed from the NUV to the I-band as part of the imaging Treasury *HST* program LEGUS: Legacy Extragalactic UV Survey. We aim to establish i) if the models provide reasonable fits to the data, ii) how well the models and photometry are able to constrain the cluster properties, and iii) how different the properties obtained with different models are.

1 Introduction

Determining extinction-corrected ages and masses for large samples of individual young massive clusters (YMCs) in a wide range of galaxy environments is essential for investigating cluster formation and evolution, characterizing the star-cluster age and mass functions of galaxies, and studying the star formation histories of galaxies (Calzetti et al. 2015). The task of observing large samples of clusters in galaxies with a wide range of properties was recently completed by *HST*'s LEGUS program (PID 13364; Calzetti et al. 2015), which consists of high spatial resolution ($\sim$ 0.07") images of portions of 50 nearby ($\leq$ 13 Mpc) galaxies taken with the UVIS channel of the Wide Field Camera Three (WFC3) in broad band filters F275W (2704 Å), F336W (3355 Å), F438W (4325 Å), F555W (5308 Å), and F814W (8024 Å). The survey includes galaxies of different morphological types and spans factors of $\sim 10^3$ in both SFR and sSFR, $\sim 10^4$ in stellar mass ($\sim 10^7 - 10^{11}\ M_\odot$), and $\sim 10^2$ in oxygen abundance (12+log(O/H)=7.2-9.2).

At the distances of LEGUS galaxies ($3-13$ Mpc), the cores of YMCs are unresolved. In such cases, a standard technique for deriving cluster properties is the comparison of observed and computed broad-band fluxes. With regards to populations of massive stars, at fixed star formation history and initial mass function (IMF), uncertainties in synthetic spectral energy distributions (SEDs) are arguably dominated by uncertainties in massive-star evolutionary tracks (Leitherer et al. 2014). In recent years, independent groups in Padova, Geneva, and Auckland, working on massive star evolution have attempted to reproduce three key observational constraints. First, the blue loops that are observed in the color-magnitude diagrams of nearby metal-poor dwarf irregular star-forming galaxies. Second, nitrogen enhancements are observed on the surfaces of main sequence stars of typically $15\ M_\odot$ (Hunter et al. 2009). Finally, it is now well established that massive stars are in binary systems with close to 70% of them interacting over the course of their evolution (Langer 2012; Sana et al. 2012; Sana et al. 2013). Processes that occur during the evolution of binaries include envelope stripping from the binary, accretion of mass by the secondary, or even complete mergers (de Mink et al. 2014). In this contribution we aim to motivate the importance of pinning down massive star evolution of which Wolf-Rayet stars are an important component.

2 Sample & Observations

We select six YMCs in galaxy NGC 1566 with ages of ≤ 50 Myr, which ensures the presence of massive stars; masses of $\geq 5\times10^4$ $M_\odot$, which mitigates the effect of the stochastic sampling of the stellar initial mass function (IMF, Cerviño & Luridiana 2004); and metallicity close to solar ($Z = 0.014$, Asplund et al. 2009), for which tracks from Padova, Geneva, and Auckland are available. Figure 1 shows the LEGUS NUV image of the galaxy and locations of clusters. We avoid the AGN at the center. We use labels from the LEGUS catalogue. The pixel scale of WFC3/UVIS is 0.039 arcsec/pixel. Photometry is performed with a circular aperture of 4 pixels in radius, with the background measured within an annulus of 7 pixels in inner radius and 1 pixel in width (for more details see Adamo et al., in prep.).

3 Models & Method

We obtain the color excess $E(B-V)$, mass $M_{\rm cl}$, and age t of individual YMCs by comparing observed and synthetic photometry in the five LEGUS bands. For the stellar component, we use instantaneous star formation, an initial stellar mass of $M_{\rm cl} = 10^6\ M_\odot$, and a Kroupa (2001) IMF in the

range $0.1-100\,M_{\odot}$. We test the most recent Padova tracks for single non-rotating stars (Bressan et al. 2012, Chen et al. 2014b in prep.), Geneva tracks for single non-rotating and single rotating stars (Ekström et al. 2012), and Auckland tracks for single non-rotating stars and interacting binary stars (Eldridge et al. in prep.). The rotating Geneva tracks are at 40% of the break-up velocity on the zero-age main sequence. None of these tracks that are mentioned so far include pre-main-sequence stars, and this should be taken as a limitation to our approach. The tracks from different cities are implemented in different spectral synthesis codes which are `Galaxev` (Bruzual & Charlot 2003; Charlot & Bruzual in prep.), `Starburst99` (Leitherer et al. 1999; Leitherer et al. 2014), and `BPASS` (Eldridge et al. in prep.), respectively. Hereafter we refer to models that use these tracks as Pn, Gn, Gr, An, and Ab, respectively. In addition to the evolution tracks, a main ingredient of spectral population synthesis are the spectra of the individual stars, which in our case are theoretical. Given that we use low-resolution spectra in order to compute broad-band fluxes, we do not expect differences in atmospheres to significantly affect our results. For Wolf-Rayet stars, all models use the PoWR models (Gräfener et al. 2002; Hamann & Gräfener 2003; Hamann & Gräfener 2004). For the nebular component we use version 13.03 of photoionization code `Cloudy` and parameters as in Zackrisson et al. (2011). We attenuate the model SEDs using the Milky Way extinction curve of Mathis (1990), a foreground dust geometry, and equal attenuation of the nebular gas and stellar continuum. The range of $E(B-V)$ values is from 0 to 3, in steps of 0.01 mag, while it is 6 to 9 in steps of 0.1 for $\log(t/\mathrm{yr})$. Thus, for a given metallicity (Z), IMF, and set of tracks, the number of models is 9331. We use Bayesian inference to derive the cluster properties. The cluster mass is a normalization constant between the observation and model. For each cluster property, i.e., $E(B-V)$, $M_{\rm cl}$, and t we record two values, the best-fit or minimum χ^2 value, and the median of the marginal probability distribution function. We use flat priors in $E(B-V)$, $\log(M_{\rm cl})$, and $\log(t)$. Our errors around the median correspond to the 16th and 84th percentiles.

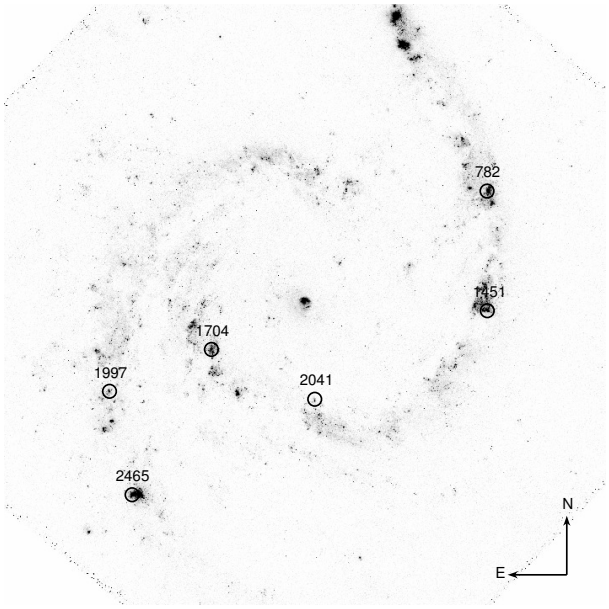

Fig. 1: F275W LEGUS image of NGC 1566. We mark the locations of clusters with circles of radius 1.6" or ∼100 pc. Photometry was extracted from circles of radius 10 times smaller. North is up and east is to the left.

4 Summary of Results

i) How well do the models fit the data? 5/6 clusters show very similar spectral shapes, except for the most reddened one. We find that for all clusters, best-fit models based on any of the tracks are able to fit the observations within the observational error bar in at least 3/5 of bands. Thus, overall the models are successful in fitting the LEGUS data. In addition, surprisingly, there is a slight preference for the Ab (binary models), which present the most degrees of freedom.

ii) How well do the models constrain the cluster properties given the data? Overall, the marginal PDFs of $E(B-V)$ are single peaked and this is the best constrained quantity. A few exceptions are the PDFs of clusters 1997 and 2041 derived from Gn or Gr models, which present multiple peaks. For the masses and ages, the marginal PDFs present multiple peaks more frequently, but there are cases were these properties are well constrained.

iii) How different are the properties obtained with the different models? Based on medians of the PDFs, the ranges of $E(B-V)$, $M_{\rm cl}$, and t found for the six clusters follow: $E(B-V) = 0.02-0.63$ mag, $M_{\rm cl}/10^4\,M_{\odot} = 1.9-11.0$, and $t/\mathrm{Myr} = 2-5$. For comparison, the ranges of properties derived from older standard models used to select the clusters are: $E(B-V) = 0.0-0.76$ mag, $M_{\rm cl}/10^4\,M_{\odot} = 5.9-14.2$, and $t/\mathrm{Myr} = 1-15$. Figures 2 to 4 show comparisons between the median values of $E(B-V)$, $M_{\rm cl}$, and t derived with the different models. Since there is a slight preference for the Ab models, we plot the Ab models on the x-axis. For $E(B-V)$, all models agree on which is the most reddened cluster. In addition, in general, models are in agreement with each other within the model error-bars. We note that Gr models are systematically offset relative to the Ab models, and yield larger values of $E(B-V)$. For $M_{\rm cl}$, all models agree on which are the least and most massive clusters, but the models are in general disagreement on the absolute value of the cluster mass within the model error bars. In addition, the

Ab models result in lower masses relative to the rest of models except the Gr models. Finally, for age, all models agree on which are the youngest (2041) and oldest (1704). The youngest is also the most reddened, which makes sense if the cluster is still partially enshrouded in its natal cloud. Wether the models agree on the ages within the model error bars depends on the cluster and pair of models. The Gr models clearly yield the oldest ages.

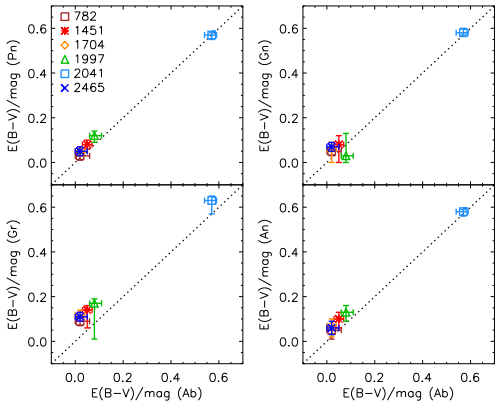

Fig. 2: Comparison of median $E(B-V)$ values obtained with models that use different massive-star evolutionary tracks. The different symbols represent the different clusters, as indicated in the legend. On the x-axis, we always plot results based on the Ab models. On the y-axis, we plot results based on the Pn, Gn, Gr, or An models, depending on the panel.

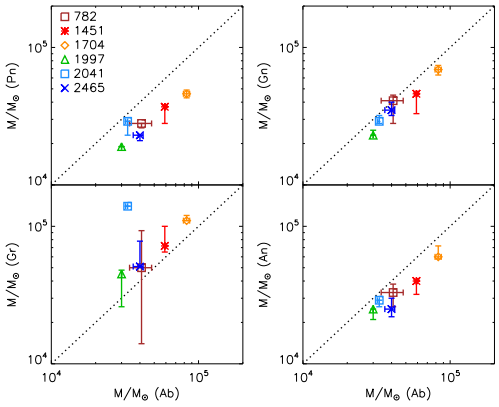

Fig. 3: Similar to Figure 2 but for the mass of clusters.

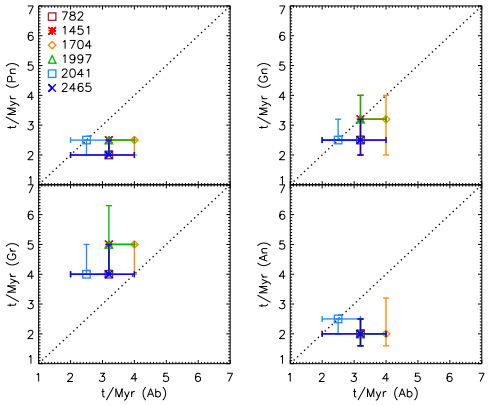

Fig. 4: Similar to Figure 2 but for the age of clusters.

A. Wofford acknowledges support from the ERC via an Advanced Grant under grant agreement no. 321323-NEOGAL.

References

Asplund, M., Grevesse, N., Sauval, A. J., & Scott, P. 2009, ARA&A, 47, 481
Bressan, A., Marigo, P., Girardi, L., et al. 2012, MNRAS, 427, 127
Bruzual, G. & Charlot, S. 2003, MNRAS, 344, 1000
Calzetti, D., Lee, J. C., Sabbi, E., et al. 2015, AJ, 149, 51
Cerviño, M. & Luridiana, V. 2004, A&A, 413, 145
de Mink, S. E., Sana, H., Langer, N., Izzard, R. G., & Schneider, F. R. N. 2014, ApJ, 782, 7
Ekström, S., Georgy, C., Eggenberger, P., et al. 2012, A&A, 537, A146
Gräfener, G., Koesterke, L., & Hamann, W.-R. 2002, A&A, 387, 244
Hamann, W.-R. & Gräfener, G. 2003, A&A, 410, 993
Hamann, W.-R. & Gräfener, G. 2004, A&A, 427, 697
Hunter, I., Brott, I., Langer, N., et al. 2009, A&A, 496, 841
Langer, N. 2012, ARA&A, 50, 107
Leitherer, C., Ekström, S., Meynet, G., et al. 2014, ApJS, 212, 14
Leitherer, C., Schaerer, D., Goldader, J. D., et al. 1999, ApJS, 123, 3
Mathis, J. S. 1990, ARA&A, 28, 37
Sana, H., de Koter, A., de Mink, S. E., et al. 2013, A&A, 550, A107
Sana, H., de Mink, S. E., de Koter, A., et al. 2012, Science, 337, 444
Zackrisson, E., Rydberg, C.-E., Schaerer, D., Östlin, G., & Tuli, M. 2011, ApJ, 740, 13

Dominik Bomans: Did I understand correctly, that the oldest and most massive cluster is the most reddened? Would one not expect that massive older clusters would clear out of dust?

Adia Wofford: The oldest and most massive is not the most reddened one.

Kimberly Sokal: Why did you choose an upper mass cutoff of $100\,M_{\odot}$? Isn't that rather low for these clusters?

Adia Wofford: The choice of the upper mass limit was driven by the fact that the standard models used by the LEGUS collaboration use an upper mass limit of $100\,M_{\odot}$. For easier comparison with these models, we also adopted $100\,M_{\odot}$ for the rest of the models.

Dorottya Szécsi: How do you know that the difference of your output (the factor 2 and 3) is attributed to the difference between the stellar evolutionary models and not to that between the stellar atmosphere models?

Adia Wofford: We use low resolution spectra to compute the magnitutes in LEGUS filters. In addition, the LEGUS filters are broad-band filters. Differences in the ionizing fluxes predicted by different massive star evolutionary tracks have a bigger effect on the predicted magnitutes.

Aida Wofford (r.) after her talk, passing the microphone to Jose Groh (l.)